Stabilizing contributions of sulfur-modified nucleotides: crystal structure of a DNA duplex with 2′-O-[2-(methoxy)ethyl]-2-thiothymidines

Benjamin Diop-Frimpong, Thazha P. Prakash[1], Kallanthottathil G. Rajeev[2], Muthiah Manoharan[2] and Martin Egli[3,*]

Department of Chemical Engineering, School of Engineering, Vanderbilt University, Nashville, TN 37235, USA, [1]Department of Medicinal Chemistry, Isis Pharmaceuticals Inc., Carlsbad, CA 92008, USA, [2]Drug Discovery, Alnylam Pharmaceuticals Inc., Cambridge, MA 02142 USA and [3]Department of Biochemistry, School of Medicine, Vanderbilt University, Nashville, TN 37232, USA

ABSTRACT

Substitution of oxygen atoms by sulfur at various locations in the nucleic acid framework has led to analogs such as the DNA phosphorothioates and 4′-thio RNA. The phosphorothioates are excellent mimics of DNA, exhibit increased resistance to nuclease degradation compared with the natural counterpart, and have been widely used as first-generation antisense nucleic acid analogs for applications *in vitro* and *in vivo*. The 4′-thio RNA analog exhibits significantly enhanced RNA affinity compared with RNA, and shows potential for incorporation into siRNAs. 2-Thiouridine (s^2U) and 5-methyl-2-thiouridine (m^5s^2U) are natural nucleotide analogs. s^2U in tRNA confers greater specificity of codon–anticodon interactions by discriminating more strongly between A and G compared with U. 2-Thio modification preorganizes the ribose and 2′-deoxyribose sugars for a C3′-*endo* conformation, and stabilizes heteroduplexes composed of modified DNA and complementary RNA. Combination of the 2-thio and sugar 2′-O-modifications has been demonstrated to boost both thermodynamic stability and nuclease resistance. Using the 2′-O-[2-(methoxy)ethyl]-2-thiothymidine (m^5s^2Umoe) analog, we have investigated the consequences of the replacement of the 2-oxygen by sulfur for base-pair geometry and duplex conformation. The crystal structure of the A-form DNA duplex with sequence GCGTAT*ACGC (T* = m^5s^2Umoe) was determined at high resolution and compared with the structure of the corresponding duplex with T* = m^5Umoe. Notable changes as a result of the incorporation of sulfur concern the base-pair parameter 'opening', an improvement of stacking in the vicinity of modified nucleotides as measured by base overlap, and a van der Waals interaction between sulfur atoms from adjacent m^5s^2Umoe residues in the minor groove. The structural data indicate only minor adjustments in the water structure as a result of the presence of sulfur. The observed small structural perturbations combined with the favorable consequences for pairing stability and nuclease resistance (when combined with 2′-O-modification) render 2-thiouracil-modified RNA a promising candidate for applications in RNAi.

INTRODUCTION

Chemically modified nucleic acids have been studied extensively in the context of the development of antisense therapeutics (1,2) and more recently in the search for small interfering RNAs (siRNAs) for *in vitro* and *in vivo* applications (3,4). In both cases, increases in RNA affinity as a result of modification can be expected to play an important role in the improvement of the efficacy of putative oligonucleotide therapeutics (5). Phosphorothioate DNA (PS-DNA) (6) has undergone extensive tests in numerous clinical trials of antisense oligonucleotides (7). In PS-DNA, one of the non-bridging phosphate oxygen atoms is replaced by sulfur. Although this altered chemistry leads to a slight reduction in RNA affinity relative to DNA, PS-DNA was considered a promising first-generation antisense modification for a number of reasons, including ease of synthesis, increased nuclease resistance

---

*To whom correspondence should be addressed. Tel: +1 615 343 8070; Fax: +1 615 322 7122; Email: martin.egli@vanderbilt.edu

and binding to proteins (biodistribution) as well as degradation of RNA bound to PS-DNA by RNase H (8). Another sulfur modification, 2-thiouridine (s^2U) was found to strongly increase the melting temperature (T_m) of heteroduplexes between modified strands and RNA compared with the corresponding DNA:RNA hybrids (9). For example, incorporation of a single s^2U residue in the center of a nonamer DNA strand led to an increase of 9.4°C in the T_m for the duplex with the complementary RNA strand compared with the unmodified hybrid duplex (10). Consecutive and interspersed replacement of several thymidines by 2′-O-[2-(methoxy)ethyl]-2-thiothymidine (m^5s^2Umoe; Figure 1) furnished an average gain in T_m of 3.5 and 3°C, respectively, for heteroduplexes between modified strands and RNA relative to the native duplexes (11).

The s^2U modification occurs naturally in transfer RNAs [(12–14); see also the RNA modification database http://medstat.med.utah.edu/RNAmods/]. The modification is present at the first position of the anticodon, position 34, and affects the relative stabilities of pairing with A and the wobble pairing with G of codons, thereby stabilizing and increasing the specificity of codon–anticodon interactions. Because sulfur
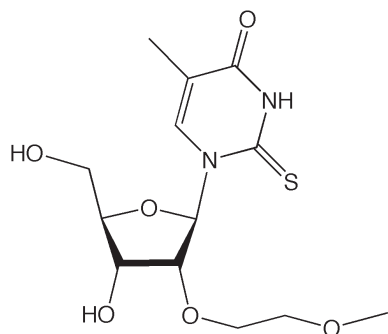
has a bigger atomic radius and lower electronegativity than oxygen, its H-bonding ability is weaker relative to the latter. As a result, the interaction between the sulfur in the 2-position of s^2U with the hydrogen on N1 of G (Figure 2A, right) is weakened compared with the corresponding pair between U and G (Figure 2B, right). On comparison, the hydrogen bond between N1 of A and N3-H of s^2U (Figure 2A, left) is only indirectly affected, rendering its stability similar to that of the U:A pair (Figure 2B, left). In summary, in the absence of the sulfur modification, the more electronegative oxygen in the 2-position of U will readily form a hydrogen bond with the hydrogen on N1 of G. This makes the U:G interaction more similar to the U:A interaction (Figure 2B) compared with the relative stability of the s^2U:G and s^2U:A pairs (Figure 2A) [(15) and cited references]. In addition to conferring pairing specificity, the s^2U modification also restricts uridine dynamics by locking the nucleoside in the *anti*, C3′-*endo* conformation (16,17). Moreover, the conformational effects of the modification extend into the 3′-adjacent nucleosides, causing them to assume a similar conformation (18,19). The strong conformational preorganization towards the C3′-*endo* pucker by the sulfur at the 2-position of the base is consistent with the aforementioned increased RNA affinity exhibited by oligonucleotides containing the s^2U modification.

To examine the potential conformational changes in a duplex as a consequence of replacement of T by m^5s^2U and to better understand the origins of the enhanced stability of s^2U-modified duplexes compared with their native counterparts, we determined the X-ray crystal structure of an A-form DNA decamer duplex with sequence 5′-GCGTA(m^5s^2Umoe)ACGC and two 2′-O-[2-(methoxy)-ethyl]-2-thiothymidine residues. The structure of the duplex with the same sequence containing a single 2′-O-[2-(methoxy)-ethyl]-thymidine per strand (5′-GCGTA(m^5Umoe)ACGC) had previously been determined at a similar resolution and was used as the reference (20). The 2′-O-MOE RNA analog is

Figure 1. Structure of 2′-O-[2-(methoxy)ethyl]-2-thiothymidine (s^2m^5Umoe).
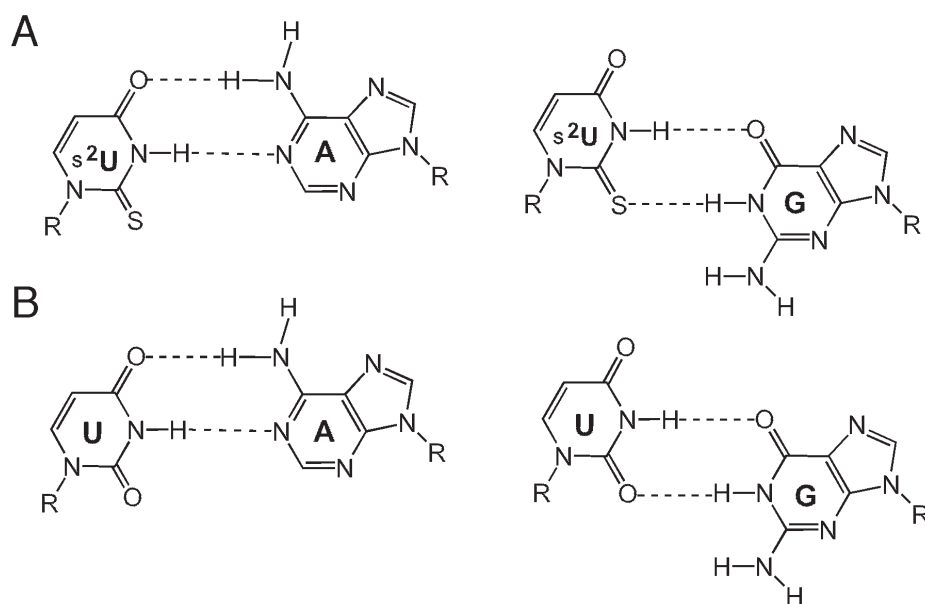

Figure 2. Pairing of U and s^2U with A and G. (**A**) Diagram illustrating s^2U base-pairing with both A and G; s^2U favors A over G. (**B**) Diagram illustrating the lack in specificity with uridine; U binds with similar affinity to both A and G.

a promising second-generation antisense modification that leads to significant gains in RNA affinity as well as enhanced nuclease resistance compared with DNA or PS-DNA (21,22). The roles of conformational preorganization, stereoelectronic effects and hydration in the stability increases afforded by the 2′-*O*-MOE modification have been studied extensively using crystallographic data obtained for partially (20) and all-2′-*O*-modified duplexes (23).

Here, we show that the presence of sulfur at the 2-position of T results in subtle changes in the local helical parameters and goes along with a slight improvement of the stacking interactions with adjacent bases, evident from the comparison of the orientations of the m^5s^2U and m^5U bases relative to their nearest neighbors in the m^5s^2Umoe-modified and reference duplex, respectively. Overall the structural data are consistent with the significant gains in thermodynamic stability afforded by the s^2U modification.

MATERIALS AND METHODS

Synthesis of the 2-thio-2′-*O*-MOE-5-methyluridine modified oligonucleotide

The 5′-*O*-DMT-2′-*O*-MOE-2-thiothymidine-3′-phosphor-amidite was prepared according to the published procedure (11). The oligonucleotide d(GCGTA)-m^5s^2Umoe-d(ACGC) was synthesized on functionalized controlled pore glass (CPG) on an automated solid phase DNA synthesizer with final DMT group retained at the 5′ end. Standard phosphor-amidites and solid supports were used for incorporation of A, T, G and C residues. A 0.1 M solution of the amidites in anhydrous acetonitrile was used for the synthesis of the modified oligonucleotide. For incorporation of 2-thio-2′-*O*-MOE-5-methyl U amidite, 6 equivalents of phosphoramidite solution were delivered in two portions, each followed by a 5 min coupling wait time. All other steps in the protocol supplied by the manufacturer were used without modification. Oxidation of the internucleotide phosphite to the phosphate was carried out using *tert*-butyl hydroperoxide/acetonitrile/water (10:87:3) with 10 min oxidation wait time. The stepwise coupling efficiencies were >97%. After completion of the synthesis, the solid support was suspended in aqueous ammonium hydroxide (30 wt%) and kept at room temperature for 2 h. The solid support was filtered and the filtrate was heated at 55°C for 6 h to complete the removal of all protecting groups. The crude oligonucleotide was purified by high performance liquid chromatography (HPLC, C-4 column, Waters, 7.8 × 300 mm, 15 μm, 300 Å, buffer A = 100 mM ammonium acetate, pH 6.5–7, buffer B = acetonitrile, 5–60% of B in 55 min, flow 2.5 ml min^{-1}, λ 260 nm). Detritylation was achieved by adjusting the pH of the solution to 3.8 with acetic acid and keeping at room temperature until complete removal of the trityl group, as monitored by HPLC analysis. The oligonucleotide was then desalted by HPLC and characterized by ES-MS (calculated mass: 3118.35 g mol^{-1}; found: 3119.57 g mol^{-1}) and purity (91% full length) was assessed by capillary gel electrophoresis.

Crystallizations and data collection

Crystallization trials were performed with the Nucleic Acid Mini-screen (24) by Hampton Research (Aliso Viejo, CA),

Table 1. Selected crystal data, data collection and refinement statistics

Crystal data	
Space group	$P2_12_12_1$
a (Å)	25.25
b (Å)	45.00
c (Å)	44.97
Data collection	
Source/detector	DND-CAT 5-ID (APS)/MAR225
Temperature (°C)	−170
Wavelength (Å)	0.9873
Total no. of reflections	51 837
No. of unique reflections	6304
Resolution range (Å)	32.0–1.61
Completeness, all/1.71–1.61 Å (%)	95.0/88.2
R-merge, all/1.71–1.61 Å (%)	7.1/15.5
Refinement statistics	
No. of DNA atoms	460
No. of water molecules	160
R.m.s. distances (Å)	0.01
R.m.s. angles (°)	2.4
Mean B value (overall, Å^2)	9.1
R-work	0.195
R-free	0.202

using the hanging drop vapor diffusion technique. Droplets with volume 2 μl of a 1:1 mixture of sample and mini-screen buffer were equilibrated against 1 ml of 35% 2-methyl-2,4-pentanediol (MPD). Crystals were obtained from a droplet that contained 1 mM oligonucleotide, 40 mM sodium cacodylate pH 7.0, 12 mM spermine tetrahydrochloride, 12 mM sodium chloride, 80 mM potassium chloride and 10% v/v MPD. A single crystal was mounted in a nylon loop and frozen in liquid nitrogen. Diffraction data were collected at low temperature in a cold nitrogen stream on the 5-ID beamline of the DuPont-Northwestern-Dow Collaborative Access Team at the Advanced Photon Source, Argonne, IL. Separate data sets for high and low resolution reflections were acquired. All data were processed with the program XDS (25) and a summary of selected crystal data and data collection statistics is listed in Table 1.

Crystal structure determination and refinement

Due to the close similarity between two of the unit cell constants, the diffraction data were processed both in the space groups *P*222 (orthorhombic) and *P*422 (tetragonal). The resulting values for *R*-merge differed only minimally (<1%) and structure determination was subsequently attempted in $P2_12_12_1$, the space group found for the vast majority of crystals of A-form DNA 10mers with isolated 2′-*O*-modified residues investigated in our laboratory (20), and in space group $P4_22_12$. Phasing was carried out by the molecular replacement method using the program AMORE (26) as part of the CCP4 suite of crystallographic programs (27). An A-form DNA decamer of the same sequence GCGTATAGCG (28) was used as the search model. Promising solutions with good R-factors, reasonable correlation coefficients, and few short lattice contacts were found in both space groups. Initial refinements of the models were performed with the program CNS (29), setting aside 5% randomly selected reflections for calculating the *R*-free (30). While the *R*-factor calculated for the model in the orthorhombic space group $P2_12_12_1$ dropped rapidly, it failed
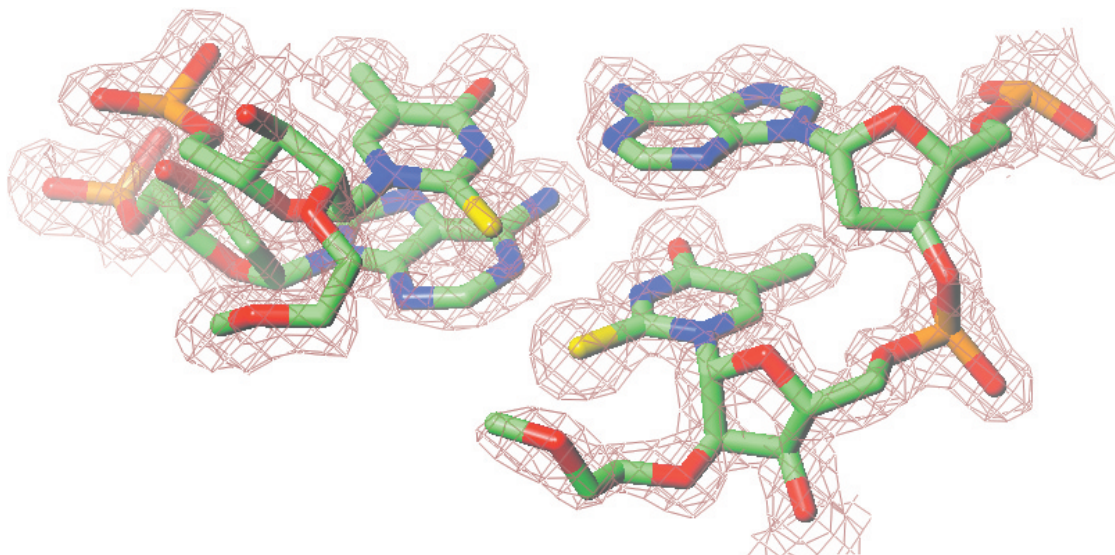
Figure 3. Example of the final sum ($2F_o$-F_c) Fourier electron density (1σ threshold) around the base-pair step (A5)p(m^{5}s^{2}Umoe6):(A15)p(m^{5}s^{2}Umoe16). The view is into the minor groove with $2'$-O-MOE substituents in the foreground (m^{5}s^{2}Umoe6, left, and m^{5}s^{2}Umoe16, right), and atoms are colored green, blue, red, orange and yellow for carbon, nitrogen, oxygen, phosphorus and sulfur, respectively.

to drop below 35% in space group $P4_22_12$. Consequently, refinement was continued only in $P2_12_12_1$. After rigid-body refinement and simulated annealing plus multiple rounds of positional and individual B-factor refinement, the complete model, including the 2-thio and $2'$-O-MOE modifications for the two modified residues, exhibited an R-factor of 30.1% (R-free of 28.5%). Refinement was then continued with the progam REFMAC (31), using a bulk solvent correction and treating DNA atoms and water molecules with restraint anisotopic B-factors (32,33). The final model refined to an R-factor of 19.4%, using all reflections up to a resolution of 1.61 Å. Selected refinement parameters are listed in Table 1 and an example of the quality of the final Fourier sum ($2F_o$-F_c) electron density is depicted in Figure 3.

Coordinates

Final coordinates and structure factors have been deposited in the Protein Data Bank (http://www.rcsb.com) PDB ID code 2AXB.

RESULTS

Overall structure

Owing to the similar b and c unit cell constants (Table 1), diffraction data from a single crystal of the m^{5}s^{2}Umoe-modified DNA decamer were indexed and processed both in orthorhombic and tetragonal space groups. Following structure determination with molecular replacement using an A-form model, initial rounds of refinement in the space groups $P2_12_12_1$ and $P4_22_12$ indicated that the crystal system is orthorhombic. Thus, the crystallographic asymmetric unit consists of a single duplex and the lattice features a non-crystallographic 4-fold symmetry. Multiple rounds of coordinate and temperature factor refinements and simulated annealing led to an improved model, and electron density

maps based on it revealed ordered $2'$-O-MOE substituents in the minor groove. The positions of sulfur atoms were marked by spherical peaks of density that are clearly enlarged relative to those around the exocyclic O4 and O2 atoms of unmodified thymines (Figure 3). In the duplex, residues of one strand are numbered from 1 to 10, and those in the complementary strand are numbered from 11 to 20; m^{5}s^{2}Umoe residues are located at positions 6 and 16.

The modified duplex adopts an A-form conformation with an average helical rise of 2.64 Å (SD 0.69 Å) an average helical twist of 34.3° (SD 3.4°). The average inclination of base pairs relative to the helical axis is 15.6°. Except for residues at the $5'$-terminal ends, the conformations of all sugars fall into the C3$'$-*endo* range. The deoxyriboses of residues G1 and C2 adopt C2$'$-*exo* and C4$'$-*exo* puckers, respectively, and G11 is flipped into the C2$'$-*endo* conformation. Similarly, most of the backbone torsion angle conformations observed in the decamer duplex are those typically associated with an A-form geometry (-*sc*/*ap*/*sc*/*sc*/*ap*/-*sc*; α to ζ). Exceptions are constituted by A5 in strand 1 and G13 in strand 2 that both assume an extended backbone variant with α, β and γ in the *ap* conformation. The conformation is brought about by a crankshaft motion of the backbone and is accompanied by elongated distances between adjacent intra-strand phosphorus atoms (6.9 Å between A5 and m^{5}s^{2}Umoe6 and 6.4 Å between G13 and T14; avg P$\cdots$P distance: 6.1 Å).

To analyze the geometry of the m^{5}s^{2}Umoe-modified duplex further and to determine potential changes as a result of the presence of sulfur atoms in the central A:m^{5}s^{2}Umoe base pairs, we used the previously determined structure of the duplex with identical sequence and m^{5}Umoe residues at positions 6 and 16 as a reference (20). The resolution of that structure is similar (1.93 Å) to that of the m^{5}s^{2}Umoe-modified duplex described here. Both crystals belong to space group $P2_12_12_1$ and have very similar cell constants [$a = 24.93$, $b = 44.59$, $c = 45.38$ Å (reference) versus $a = 25.25$, $b = 45.00$, $c = 44.97$ Å]. We will refer to the reference

and the 2-thio-modified duplexes as the m^{5}Umoe and m^{5}s^{2}Umoe structures, respectively.

Crystal packing effects

Because the conformational perturbations caused by the 2-thio modification can be expected to be quite subtle, it is important to identify and quantify conformational differences between the m^{5}s^{2}Umoe-modified and reference duplexes that are due to crystal packing effects. Interactions between neighboring duplexes in the crystal lattices of m^{5}Umoe and m^{5}s^{2}Umoe decamers involve stacking of terminal base pairs into the outer portions of the minor groove (34). This particular mode of interaction triggers various degrees of kinking into the major groove. Individual crystallization conditions, the chemistry and spatial properties of substituents of 2′-O-modified residues and their location in the decamer strand, as well as data collection temperature all appear to play a role in the relative degree of kinking (35). Superimposition of the two duplexes reveals that the m^{5}Umoe decamer exhibits a slightly stronger kink than the m^{5}s^{2}Umoe decamer (Figure 4).
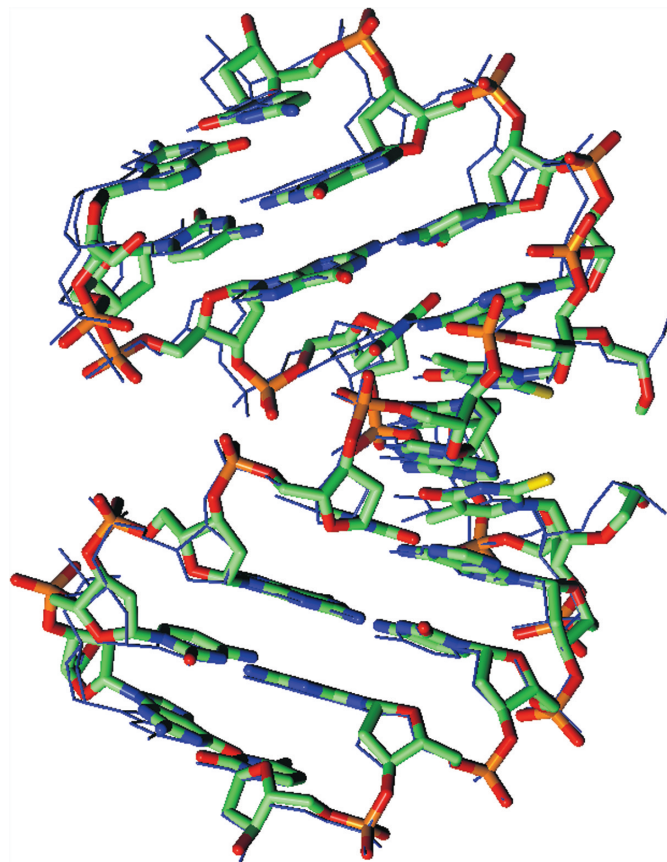

Figure 4. Overall conformation of the m^{5}s^{2}Umoe-modified decamer (atoms are colored green, blue, red, orange and yellow for carbon, nitrogen, oxygen, phosphorus and sulfur, respectively) compared with the m^{5}Umoe-modified reference duplex (thin blue lines). The view of the A-form duplexes is across the major (top) and minor grooves (bottom) and the 5′-terminal G1 and G11 residues are located at the top left and bottom left, respectively. 2′-O-Substituents are jutting into the minor groove and 2-sulfur atoms highlighted in yellow. The reduced kink into the major groove in the m^{5}s^{2}Umoe-modified decamer between the tetramer 5′-G1pC2pG3pT4:3′-C20pG19pC18pA17p and the hexamer 5′-pA5p(m^{5}s^{2}Umoe6)pA7pC8pG9pC10:3′-(m^{5}s^{2}Umoe16)-pA15pT14pG13pC12pG11 is clearly visible.

The kink compresses the major groove and occurs between the tetramer 5′-G1pC2pG3pT4 and the hexamer pA5p(m^{5}U-moe6)pA7pC8pG9pC10. It is accompanied by significant changes in the local base-pair (stagger), base-pair step (rise, twist and roll) and base-pair helical parameters (inclination). The absolute values of these parameters at that site constitute either the minimum (stagger [m^{5}Umoe], rise, twist) or maximum (stagger [m^{5}s^{2}Umoe], roll, inclination) among the individual observations with both duplexes. Most probably, these changes are only weakly affected by the oxygen→sulfur substitution in residue 16, although the kink occurs between the T4:A17 and A5:m^{5}s^{2}Umoe16 pairs. Rather, they are a reflection of the intrinsic conformational properties ('bendability') of the decamer sequence and the packing forces in the orthorhombic crystal lattice. Regarding the possible origins of the observed difference in kinking in the two duplexes, it is noteworthy that the m^{5}Umoe structure was determined at room temperature (20) whereas the m^{5}s^{2}Umoe structure is derived from diffraction data collected at −170°C. Thus, slightly divergent packing forces due to the temperature change are the most likely cause of the observed differences between the global conformations of the m^{5}s^{2}Umoe and m^{5}Umoe duplexes. Because of the kink adjacent to the A5:m^{5}s^{2}Umoe16 base pair and the ensuing perturbations in its immediate vicinity, one would expect that careful analysis of the geometry of the other modified base pair, m^{5}s^{2}Umoe6:A15, might yield a more reliable estimate of the changes as a result of the 2-thio modification.

Effects of the 2-thio modification on the local conformation

Both structures were analyzed with the program 3DNA that allows calculation of geometric parameters for nucleic acid molecules (36). Among the parameters, one would expect those that concern the local geometry of base pairs and the stacking interactions to be the most informative in terms of potential conformational changes due to 2-thio modification. Figure 5 depicts graphic representations of selected geometric parameters for base pairs in the m^{5}s^{2}Umoe and reference duplexes. A significant change (11°) is observed in the parameter opening for base pair m^{5}s^{2}Umoe6:A15 compared with the corresponding pair in the reference structure (Figure 5A). This change in opening results in a larger separation between the C2 atoms of the two bases in the minor groove with the 2-thio modified pair [4.23 Å versus 3.89 Å (ref. structure); Figure 6A]. Comparison of the stretch parameters also indicates a small change (0.15 Å; not shown) for this base pair that is related to accommodating the larger sulfur atom. Compared with the above change in opening, the differences in the parameters shear, stagger and propeller twist (Figure 5B–D, respectively) are relatively minor for base pair m^{5}s^{2}Umoe6:A15. Likewise, it does not appear that buckling of bases is affected by the sulfur substitution. The calculated values for both the m^{5}s^{2}Umoe6:A15 and the A5:m^{5}s^{2}Umoe16 pairs differ by <1° from those for the corresponding pairs in the reference structure. Interestingly, the latter base pair does not exhibit an altered opening angle relative to the reference duplex (Figure 5A). The difference amounts to less, ∼2° although the separation between C2 atoms of bases (4.11 Å) is comparable with that seen in

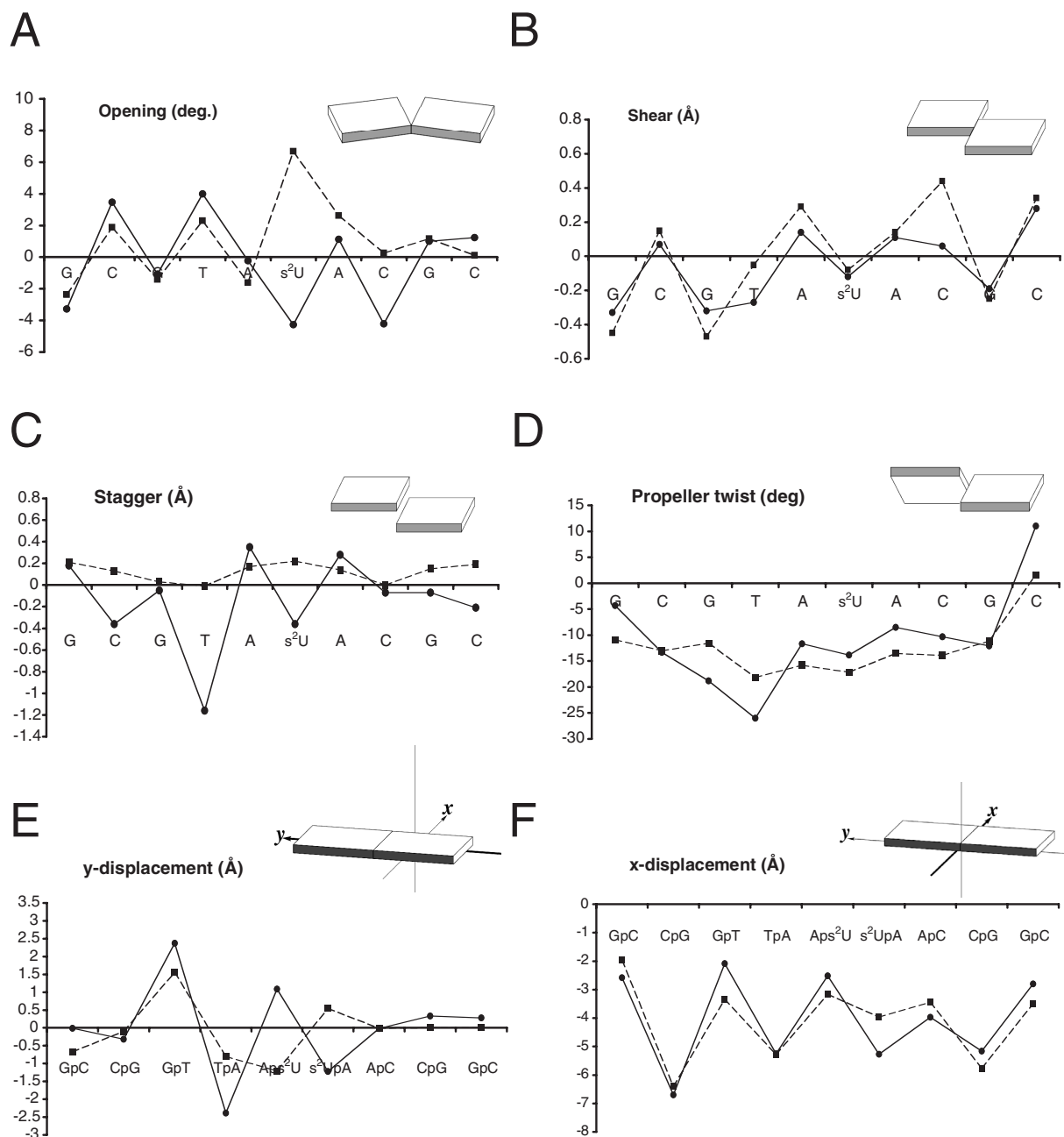**Figure 5.** Local inter-base parameters (**A**) 'opening', (**B**) 'shear', (**C**) 'stagger' and (**D**) 'propeller twist', and local base-pair helical parameters (**E**) 'y-displacement' and (**F**) 'x-displacement' in the m^5s^2Umoe- (filled circles, thin solid lines) and m^5Umoe-modified decamer duplexes (filled squares, dashed lines). All parameters were calculated with the program 3DNA (36) and a cartoon of the particular parameter is shown at the upper right in each panel.

the m^5s^2Umoe6:A15 pair (see above). Similarly, other parameters, including stretch, shear, stagger and propeller twist change subtly, but none of them appears to be making the major contribution such as opening in case of the m^5s^2Umoe6:A15 pair (Figure 5). Rather, the combination of many small changes results in an arrangement that shifts the sulfur atom away from the C2 atom of adenine in the minor groove. In any case, a superposition of the s^2m^5Umoe6:A15 and A5:s^2m^5Umoe16 pairs demonstrates that they adopt relatively similar conformations, with virtually

identical relative orientations of C2(A) and S2(m^5s^2Umoe) (Figure 6B).

In order to examine whether presence of the sulfur atoms in the m^5s^2Umoe structure led to changes in the stacking interactions involving the four central base pairs, we calculated the overlap areas between adjacent pairs in $\mathring{A}^2$ units (36). The 3DNA program allows computation of the surface areas of polygons projected in the mean plane of a base pair at a particular step, including exocyclic ring atoms. Stacking interactions at selected base-pair steps are shown in Figure 7.
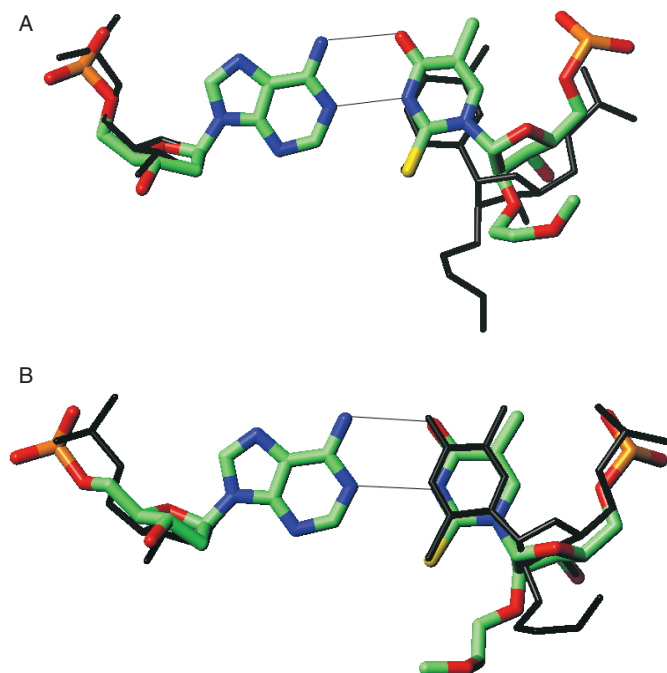
Figure 6. Effects of the 2-thio modification on the geometry of m^5s^2Umoe:A base pairs. (**A**) Superimposition of the m^5s^2Umoe6:A15 (colored by atom) and m^5Umoe6:A15 (black lines) base pairs, illustrating base opening in the m^5s^2U-moe:A base pair. (**B**) Superimposition of the A5:m^5s^2Umoe16 (colored by atom) and m^5s^2Umoe6:A15 (black lines) base pairs, illustrating the nearly identical orientations of the C2(A) and S2(m^5s^2Umoe) atoms in the two pairs. The views are approximately along the normal to the base planes and Watson–Crick hydrogen bonds are drawn as thin solid lines.

Inspection of the plotted diagrams for the m^5s^2Umoe and reference duplexes reveals minor alterations in stacking at most base-pair steps. An exception is found at the (A5)p(m^5s^2Umoe6):(A15)p(m^5s^2Umoe16) step (Figure 7C) that displays a clearly visible shift between base pairs relative to the reference structure. Indeed, the calculated *y*-displacement at that site shows a difference of 2.3 Å between the m^5s^2Umoe and m^5Umoe structures (1.1 versus −1.2 Å, respectively; Figure 5E). The difference in *x*-displacement is somewhat smaller, −1.3 Å (−5.3 versus −4.0 Å in m^5s^2Umoe and m^5Umoe, respectively; Figure 5F), but consti-tutes the largest change for that parameter in the entire duplex. The two neighboring steps also show considerable changes in *y*-displacement that amount to −1.6 Å (Figure 7B) and −1.7 Å (Figure 7D). At the central step, it is readily apparent that the two sulfur atoms have moved toward one another. Indeed, the distance between the sulfur atoms (3.48 Å) is shorter than the one between the corresponding O2 atoms in the reference structure (3.73 Å). The former is slightly shorter than the sum of van der Waals radii for the two sulfur atoms (3.6 Å). When the overlap areas between adjacent base pairs at the (T4)p(A5):(m^5s^2Umoe16)p(A17), (A5)p(m^5s^2Umoe6):(A15)p(m^5s^2Umoe16) and (m^5s^2Umoe6) p(A7):(T14)p(A15) steps (Figure 7B–D) are added, a slight increase in stacking for the m^5s^2Umoe decamer compared with the reference structure is apparent (17 Å^2 versus 15 Å^2). There-fore, we can conclude that the experimental data regarding stacking are at least in line with the stabilizing effect of the 2-thio modification.

Hydration of sulfur atoms and MOE moieties

In the minor groove, sulfur atoms of adjacent m^5s^2Umoe resi-dues are bridged by a single water molecule. This water, in turn, forms a hydrogen bond to the outer oxygen of the 2′-*O*-MOE substituent of m^5s^2Umoe16, and a second, relatively weak hydrogen bond to the 4′-oxygen of the same residue. The 2-sulfur atom of m^5s^2Umoe6 is hydrogen bonded to a second water molecule. This water bridges the nucleobase to a further water molecule that is itself hydrogen bonded to both O2′ and the outer oxygen of the 2′-*O*-MOE substituent from m^5s^2Umoe6. Both 2′-*O*-MOE moieties adopt *gauche* conformations (m^5s^2Umoe6, sc^+, and m^5s^2Umoe16, sc^-, Figure 3). In the case of m^5s^2Umoe6, the substituent is directed toward the center of the minor groove, allowing for a direct link between the MOE moiety and the minor groove edge of the base by a single water molecule. On comparison, the substituent of m^5s^2Umoe16 is directed away from the base edge, therefore requiring a water tandem to link MOE moiety and S2. Water molecules trapped between the 2′- and the outer oxygen atoms of MOE substituents are connected to phosphate groups from 3′-adjacent residues via single- or double-water bridges, a particular feature previously observed in the crystal structures of 2′-*O*-MOE-modified RNAs (20,23) and shared by other modifications with 2′-*O*-substituents containing hydrogen-bond acceptors and/or donors (37). The presence of a stable network of water molecules in the minor groove that connects m^5s^2U bases with sugar moieties and phosphate groups provides an indication that the 2-thio modification does not significantly alter the water structure compared with uracil. This observation alone does not allow conclusions as to the role of hydration in the overall stabilizing effect of the 2-thio modification. Nevertheless, the absence of obvious disruptions in the minor groove hydration by sulfur atoms in the m^5s^2Umoe duplex structure clearly argues against a destabil-izing contribution.

DISCUSSION

The primary goal of the present study was an assessment of the structural perturbations induced by the 2-thio modification in an A-form duplex environment. The m^5s^2Umoe nucleoside does not occur naturally; the choice to focus on this modifica-tion rather than the natural, biologically active s^2U and m^5s^2U pyrimidines (13,38) is based on the expectation that the 2-thio modification alone will most probably not provide sufficient nuclease resistance for *in vivo* and cell-based RNAi or anti-sense applications. A facile synthesis of the m^5s^2Umoe phos-phoramidite building block for solid-phase synthesis has been reported, and, indeed, the combination of the 2-thio and 2′-*O*-MOE modifications confers increased nuclease resistance based on *in vitro* measurements of resistance against snake venom phosphodiesterase degradation (half-lives of oligos with m^5s^2Umoe modifications >24 h) (11).

Replacement of the 2-oxygen of U or T by sulfur was shown to greatly increase RNA affinity of base-modified oligonuc-leotides (9–11). The combination of the 2-thio and 2′-*O*-MOE modifications also resulted in a higher thermodynamic stabil-ity of duplexes between modified oligonucleotides and com-plementary DNA (11), albeit to a lesser extent compared with the corresponding RNAs. One would not expect a modification
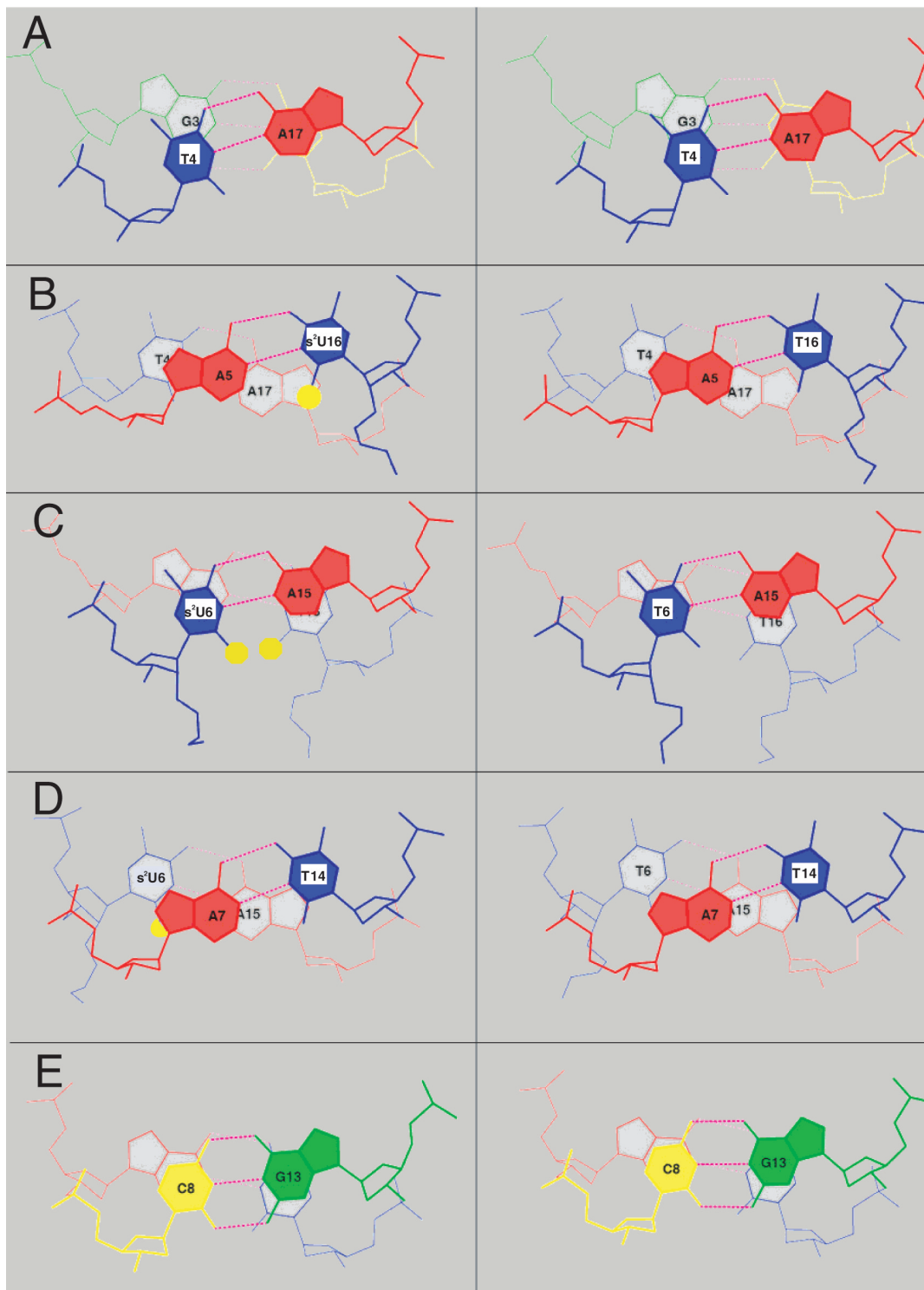
Figure 7. Improvement of stacking interactions as a result of the 2-thio modification. Panels on the left show stacking interactions in the m^{5}s^{2}Umoe-modified duplex and panels on the right show stacking interactions at the corresponding steps in the m^{5}Umoe-modified reference duplex. Base-pair steps (**A**) (G3)p(T4):(A17)p(C18), (**B**) (T4)p(A5):(m^{5}s^{2}Umoe16)p(A17), (**C**) (A5)p(m^{5}s^{2}Umoe6):(A15)p(m^{5}s^{2}Umoe16), (**D**) (m^{5}s^{2}Umoe6)p(A7):(T14)p(A15) and (**E**) (A7)p(C8):(G13)p(T14). G, C, A and T are colored green, yellow, red and blue, respectively, and sulfur atoms are highlighted as yellow spheres. The figures were generated with the program 3DNA (36).

that brings about a considerable increase in the stability of duplexes to significantly alter the geometry of the nucleobase, sugar or phosphate portions, and/or the local and global conformations of a secondary or tertiary nucleic acid structural motif. This assumption is based on observations from crystallographic data, indicating that stabilizing modifications commonly mimic the native conformation, whereas those that lead to a loss of stability often display significant deviations,

including sterically unfavorable interactions (20,39). Right from the outset of the work described here, we were aware that effects triggered by 2-thio modification would be rather subtle and hence their detection would require relatively precise structural data. The resolution of the structure of the A-form decamer duplex with m^5s^2Umoe modifications, although not extremely high, should be sufficient to ferret out some of the consequences of the 2-thio and sugar modifications for base-pair geometry and duplex conformation. Likewise, availability of a structure as a reference molecule that differs from the duplex investigated here only by the absence of the sulfur atom in the m^5Umoe residues renders the analysis more meaningful as it allows for a separation of various overlaid effects.

Key features of the m^5s^2Umoe residues in the crystal structure of the modified DNA duplex are the C3′-*endo* pucker and various subtle changes in the base pair, base-pair step and base-pair helical parameters. In addition, the sulfur atoms are in van der Waals contact across the minor groove as a result of *y*- and *x*-displacements at the central base-pair step (Figures 5 and 7C) and, judging from base overlaps in the vicinity of m^5s^2Umoe residues, 2-thio modification leads to small but measurable improvements in the stacking interactions compared with the reference structure. Among the changes in base-pair geometry, the altered opening between m^5s^2Umoe6 and A15 is readily apparent (Figures 5A and 6A). In fact, this is perhaps the most straightforward way to accommodate the larger sulfur atom opposite the C2–H2 function of adenine. Increased propeller twist, stagger or shear relative to a canonical geometry of the native T:A pair in principle could each be used separately to relieve the steric challenge posed by the larger sulfur. However, the opening seen in the m^5s^2Umoe6:A15 pair is unique in the sense that this adjustment seems sufficient alone to accommodate the sulfur atom. In contrast, it appears that, rather than relying on a single parameter to adjust to the bulkier sulfur, a combination of adjustments including all of the above parameters is responsible for generating the particular arrangement seen in the A5:m^5s^2Umoe16 pair.

Sugar pucker, nucleoside conformation and base-pair geometry are the result of a host of factors, including stereoelectronic effects. However, unlike improvements in stacking or extensive hydration networks (the structure reveals both), the structure does not allow any conclusions per se regarding either a favorable or unfavorable contribution by some of these factors to the net increase in stability observed with the m^5s^2Umoe modification. In other words, although 2-thio modification will probably cause a stronger preference of the sugar for the C3′-*endo* pucker, all we see in the structure is the product of the various stereoelectronic effects that bear on the conformation and we can only speculate as to the relative magnitude of the individual contributions toward the net gain in stability. One of these (hidden) contributions is the strengthening of the O4′–C1′–N1 anomeric effect in m^5s^2U compared with thymine (see reference (40), pp. 43–46, for a discussion of the relation between sugar pucker type and molecular orbital overlap and hyperconjugation). Because oxygen is a more electronegative element than sulfur, it may appear counter-intuitive to consider sulfur a better acceptor of negative charge than oxygen. Indeed, oxygen has a greater ability to attract electron density per unit surface area. But if the greater surface area of sulfur compared with oxygen is taken into account (factor 2.5), and the potentials for each atom are summed over their respective spherical surfaces, sulfur may well end up having an equal or greater potential than oxygen. Another effect that could contribute favorably to the higher stability afforded by the m^5s^2Umoe modification is a change in Watson–Crick hydrogen bonding strength compared with RNA A:U or DNA A:T pairs. The N1⋯N3 hydrogen bond between A:U pairs in RNA was recently shown to be stronger than the corresponding interaction in DNA (41).

With the m^5s^2Umoe nucleoside, the modulation of stereoelectronic effects extends into the 2′-*O*-substituent. For example, the *gauche* effect between O4′ and O2′ that drives the sugar conformational equilibrium toward the C3′-*endo* side is enhanced by the presence of electronegative atoms or groups in the substituent, as recently demonstrated by extensive analyses of the influence of the chemistry of RNA 2′-*O*-substituents on the stability of duplexes (37,39,42–44). Combining the 2-thio and 2′-*O*-MOE modifications generates synergistic stereoelectronic effects that are absent, e.g. in oligonucleotides modified by 2′-*O*-methyl-2-thiouridine (10). These additive effects are the basis for the high RNA affinity and increased nuclease resistance of the m^5s^2Umoe modification.

Nature's use of the s^2U and m^5s^2U pyrimidines (i.e. in tRNA) is clearly related to the conformational rigidity of their ribose moiety as a result of the substitution of the 2-oxygen by sulfur. The influence of the sulfur substitution is demonstrated by the altered binding affinity and cleavage activity of RNase H, an enzyme that is exquisitely sensitive to conformational or steric changes in DNA:RNA substrates (45). Although the enzyme binds RNA duplexes they are not recognized as substrates (46), presumably because a canonical A-form geometry precludes endonucleolytic cleavage of the RNA strand. Consistent with this observation, incorporation of m^5s^2U into the DNA strand of heteroduplexes dramatically reduced the cleavage rate at ribonucleotides opposite modified residues (47). Although this puts limitations on the use of this modification in antisense applications, where RNase H-mediated degradation of the target mRNA is considered important for efficacy, the properties of the s^2U, m^5s^2U and m^5s^2Umoe modifications may render them of interest for use in siRNAs. Together with DNA phosphorothioates (8) and 4′-thio-RNA (3,48,49), they constitute the third class of sulfur-modified nucleic acid building blocks with promising features for the generation of nucleic acid therapeutics.

REFERENCES

1. Crooke,S.T. (1998) Basic principles of antisense therapeutics. In Crooke,S.T. (ed.), *Antisense Research and Application*, Vol. 131, Springer, Berlin, pp. 1–50.
2. Manoharan,M. (1999) 2′-Carbohydrate modifications in antisense oligonucleotide therapy: importance of conformation, configuration and conjugation. *Biochim. Biophys. Acta.*, **1489**, 117–130.
3. Manoharan,M. (2004) RNA interference and chemically modified small interfering RNAs. *Curr. Opin. Chem. Biol.*, **8**, 570–579.
4. Soutschek,J., Akinc,A., Bramlage,B., Charisse,K., Constien,R., Donoghue,M., Elbashir,S., Geick,A., Hadwiger,P., Harborth,J. *et al.* (2004) Therapeutic silencing of an endogenous gene by systemic administration of modified siRNAs. *Nature*, **432**, 173–178.
5. Egli,M. (1998) Towards the structure-based design of nucleic acid therapeutics. In Weber,G. (ed.), *Advan. Enzyme Regul.* Vol. 38, Elsevier Science Ltd., Oxford, UK, pp. 181–203.
6. Levin,A.A. (1999) A review of issues in the pharmacokinetics and toxicology of phosphorothioate antisense oligonucleotides. *Biochim. Biophys. Acta.*, **1489**, 69–84.
7. Filmore,D. (2004) Assessing antisense. *Modern Drug Discovery* June, 49–50.
8. Crooke,S.T. (1995) Phosphorothioate oligonucleotides. In Crooke,S.T. (ed.), *Therapeutic Applications of Oligonucleotides*. R. G. Landes, Austin, pp. 63–79.
9. Kumar,R.K. and Davis,D.R. (1997) Synthesis and studies on the effect of 2-thiouridine and 4-thiouridine on sugar conformation and RNA duplex stability. *Nucleic Acids Res*., **25**, 1272–1280.
10. Shohda,K., Okamoto,I., Wada,T., Seio,K. and Sekine,M. (2000) Synthesis and properties of 2′-*O*-methyl-2-thiouridine and oligoribonucleotides containing 2′-*O*-methyl-2-thiouridine. *Bioorg. Med. Chem. Lett.*, **10**, 1795–1798.
11. Rajeev,K.G., Prakash,T.P. and Manoharan,M. (2003) 2′-Modified-2-thiothymidine oligonucleotides. *Org. Lett.*, **5**, 3005–3008.
12. Grosjean,H. and Benne,R. (eds) (1998) *Modification and Editing of RNA*. ASM Press, Washington, DC.
13. Rozenski,J., Crain,P.F. and McCloskey,J.A. (1999) The RNA modification database: 1999 update. *Nucleic Acids Res.*, **27**, 196–197.
14. Agris,P. (2004) Decoding the genome: a modified view. *Nucleic Acids Res.*, **32**, 223–238.
15. Testa,S.M., Disney,M.D., Turner,D.H. and Kierzek,R. (1999) Thermodynamics of RNA–RNA duplexes with 2- or 4-thiouridines: implications for antisense design and targeting of a group I intron. *Biochemistry*, **38**, 16655–16662.
16. Yokoyama,S., Watanabe,T., Murao,K., Ishikura,H., Yamaizumi,Z., Nishimura,S. and Miyazawa,T. (1985) Molecular mechanism of codon recognition by tRNA species with modified uridine in the first position of the anticodon. *Proc. Natl Acad. Sci. USA*, **82**, 4905–4909.
17. Sierzputowska-Gracz,H., Sochaka,E., Malkiewicz,A., Kuo,K., Gehrke,C.W. and Agris,P.F. (1987) Chemistry and structure of modified uridines in the anticodon, wobble position of transfer RNA are determined by thiolation. *J. Am. Chem. Soc.*, **109**, 7171–7177.
18. Agris,P.F., Sierzputowska-Gracz,H., Smith,W., Malkiewicz,A., Sochacka,E. and Nawrot,B. (1992) Thiolation of uridine carbon-2 restricts the motional dynamics of the transfer RNA wobble position nucleoside. *J. Am. Chem. Soc.*, **114**, 2652–2656.
19. Smith,W.S., Sierzputowska-Gracz,H., Sochacka,E., Malkiewicz,A. and Agris,P. (1992) Chemistry and structure of modified uridine dinucleosides are determined by thiolation. *J. Am. Chem. Soc.*, **114**, 7989–7997.
20. Tereshko,V., Portmann,S., Tay,E.C., Martin,P., Natt,F., Altmann,K.-H. and Egli,M. (1998) Correlating structure and stability of DNA duplexes with incorporated 2′-*O*-modified RNA analogues. *Biochemistry*, **37**, 10626–10634.
21. De Mesmaeker,A., Häner,R., Martin,P. and Moser,H.E. (1995) Antisense oligonucleotides. *Acc. Chem. Res.*, **28**, 366–374.
22. Martin,P. (1995) New access to 2′-*O*-alkylated ribonucleosides and properties of 2′-*O*-alkylated oligoribonucleotides. *Helv. Chim. Acta.*, **78**, 486–504.
23. Teplova,M., Minasov,G., Tereshko,V., Inamati,G.B., Cook,P.D., Manoharan,M. and Egli,M. (1999) Crystal structure and improved antisense properties of 2′-*O*-(2-methoxyethyl)-RNA. *Nature Struct. Biol.*, **6**, 535–539.
24. Berger,I., Kang,C.H., Sinha,N., Wolters,M. and Rich,A. (1996) A highly efficient 24-condition matrix for the crystallization of nucleic acid fragments. *Acta Cryst. D*, **52**, 465–468.
25. Kabsch,W. (1993) Automatic processing of rotation diffraction data from crystals of initially unknown symmetry and cell constants. *J. Appl. Cryst.*, **26**, 795–800.
26. Navaza,J. (1997) AMoRe: an automated molecular replacement program package. *Meth. Enzymol.*, **276**, 581–594.
27. CCP4. (1994), Collaborative computing project number 4. The CCP4 suite: programs for protein crystallography. *Acta Cryst. D*, **50**, 760–763.
28. Egli,M., Tereshko,V., Teplova,M., Minasov,G., Joachimiak,A., Sanishvili,R., Weeks,C.M., Miller,R., Maier,M.A., An,H., Cook,P.D. and Manoharan,M. (2000) X-ray crystallographic analysis of the hydration of A- and B-form DNA at atomic resolution. *Biopolymers (Nucleic Acid Sciences)*, **48**, 234–252.
29. Brünger,A.T., Adams,P.D., Clore,G.M., DeLano,W.L., Gros,P., Grosse-Kunstleve,R.W., Jiang,J.S., Kuszewski,J., Nilges,M., Pannu,N.S., Read,R.J., Rice,L.M., Simonson,T. and Warren,G.L. (1998) Crystallography & NMR System: a new software suite for macromolecular structure determination. *Acta Cryst. D*, **54**, 905–921.
30. Brünger,A.T. (1992) Free *R* value: a novel statistical quantity for assessing the accuracy of crystal structures. *Nature*, **355**, 472–475.
31. Murshudov,G.N., Vagin,A.A. and Dodson,E.J. (1997) Refinement of macromolecular structures by the maximum-likelihood method. *Acta. Cryst. D*, **53**, 240–255.
32. Murshudov,G.N., Vagin,A.A., Lebedev,A., Wilson,K.S. and Dodson,E.J. (1999) Efficient anisotropic refinement of macromolecular structures using FFT. *Acta Cryst. D*, **55**, 247–255.
33. Winn,M.D., Isupov,M.N. and Murshudiv,G.N. (2001) Use of TLS parameters to model anisotropic displacements in macromolecular refinement. *Acta. Cryst. D*, **57**, 122–133.
34. Egli,M., Usman,N. and Rich,A. (1993) Conformational influence of the ribose 2′-hydroxyl group: crystal structures of DNA–RNA chimeric duplexes. *Biochemistry*, **32**, 3221–3237.
35. Tereshko,V., Wilds,C.J., Minasov,G., Prakash,T.P., Maier,M.A., Howard,A., Wawrzak,Z., Manoharan,M. and Egli,M. (2001) Detection of alkali metal ions in DNA crystals using state-of-the-art X-ray diffraction experiments. *Nucleic Acids Res.*, **29**, 1208–1215.
36. Lu,X-J., Shakked,Z. and Olson,W.K. (2000) A-DNA conformational motifs in ligand-bound double helices. *J. Mol. Biol.*, **300**, 819–840.
37. Egli,M., Minasov,G., Tereshko,V., Pallan,P.S., Teplova,M., Inamati,G.B., Lesnik,E.A., Owens,S.R., Ross,B.S., Prakash,T.P. and Manoharan,M. (2005) Probing the influence of stereoelectronic effects on the biophysical properties of oligonucleotides: comprehensive analysis of the RNA affinity, nuclease resistance and crystal structure of ten 2′-*O*-ribonucleic acid modifications. *Biochemistry*, **44**, 9045–9057.
38. Lagoja,I.M. (2005) Pyrimidine as a constituent of naturally biologically active compounds. *Chemistry & Biodiversity*, **2**, 1–50.
39. Pattanayek,R., Sethaphong,L., Pan,C., Prhavc,M., Prakash,T.P., Manoharan,M. and Egli,M. (2004) Structural rationalization of a large difference in RNA affinity despite a small difference in chemistry between two 2′-*O*-modified nucleic acid analogs. *J. Am. Chem. Soc.*, **126**, 15006–15007.
40. Thibaudeau,C. and Chattopadhyaya,J. (1999) *Stereoelectronic Effects in Nucleosides and Nucleotides and their Structural Implications*. Uppsala University Press, Uppsala, Sweden.
41. Vakonakis,I. and LiWang,A.C. (2004) N1⋯N3 hydrogen bonds of A:U base pairs of RNA are stronger than those of A:T base pairs of DNA. *J. Am. Chem. Soc.*, **126**, 5688–5689.
42. Prakash,T.P., Manoharan,M., Fraser,A.S., Kawasaki,A.M., Lesnik,E., Sioufi,N., Leeds,J.M., Teplova,M. and Egli,M. (2002) 2′-*O*-[2-(Methylthio)ethyl]-modified oligonucleotide: an analog of 2′-*O*-[2-(methoxy)ethyl]-modified oligonucleotide with improved protein binding properties and high binding affinity to target RNA. *Biochemistry*, **41**, 11642–11648.
43. Prhavc,M., Prakash,T.P., Minasov,G., Egli,M. and Manoharan,M. (2003) 2′-*O*-{2-[2-(*N,N*-Dimethylamino)ethoxy]ethyl} modified antisense

oligonucleotides: symbiosis of charge interaction factors and stereoelectronic effects. *Org. Lett*., **5**, 2017–2020.

44. Prakash,T.P., Pueschl,A., Lesnik,E., Tereshko,V., Egli,M. and Manoharan,M. (2004) 2′-*O*-[2-(guanidinium)ethyl]-5-methyluridine modified oligonucleotides: synthesis and stabilizing effect on duplex and triplex nucleic acid structures. *Org. Lett*., **6**, 1971–1974.

45. Minasov,G., Teplova,M., Nielsen,P., Wengel,J. and Egli,M. (2000) Structural basis of cleavage by RNase H of hybrids of arabinonucleic acids and RNA. *Biochemistry*, **39**, 3525–3532.

46. Lima,W.F. and Crooke,S.T. (1997) Binding affinity and specificity of *Escherichia coli* RNase H1: impact on the kinetics of catalysis of antisense oligonucleotide-RNA hybrids. *Biochemistry*, **36**, 5004–5019.

47. Lima,W.F., Nichols,J.G., Wu,H., Prakash,T.P., Migawa,M.T., Wyrzykiewicz,T.K., Bhat,B. and Crooke,S.T. (2004) Structural requirements at the catalytic site of the heteroduplex substrate for human RNase H1 catalysis. *J. Biol. Chem*., **279**, 36317–36326.

48. Hoshika,S., Minakawa,N. and Matsuda,A. (2004) Synthesis and physical and physiological properties of 4′-thioRNA: application to post-modification of RNA aptamer toward NF-κB. *Nucleic Acids Res*., **32**, 3815–3825.

49. Haeberli,P., Berger,I., Pallan,P.S. and Egli,M. (2005) Syntheses of 4′-thioribonucleosides and thermodynamic stability and crystal structure of RNA oligomers with incorporated 4′-thiocytosine. *Nucleic Acids Res*., **33**, 3965–3975.